The $\gamma n \to \pi^- p$ Process from ^{2}H, ^{4}He and ^{12}C and the $\gamma p \to \pi^+ n$ Reaction (A Hall A Collaboration Experiment)

D. Dutta(Spokesperson), H. Gao(Spokesperson), K. Kramer, X. Qian, W. Xu, Q. Ye, X. Zong
TRIANGLE UNIVERSITIES NUCLEAR LAB, DUKE UNIVERSITY
J. Arrington, K. Hafidi, D.F. Geesaman, R.J. Holt(Spokesperson),
H. E. Jackson, D. H. Potterveld, P. E. Reimer, E. C. Schulte and X. Zheng.
ARGONNE NATIONAL LABORATORY
T. Averett, V. Sulkosky,
COLLEGE OF WILLIAM and MARY
M. Coman, P. Markowitz,
FLORIDA INTERNATIONAL UNIVERSITY
P. Jain,
INDIAN INSTITUTE OF TECHNOLOGY, KANPUR
B. Clasie, C. Crawford, C. J. Seely, C.F. Williamson
MASSACHUSETTS INSTITUTE OF TECHNOLOGY
R. E. Segel,
NORTHWESTERN UNIVERSITY
S. Dieterich, C. Glashausser, R. Gilman, X.D. Jiang, G. Kumbartzki, R.D. Ransome,
RUTGERS UNIVERSITY
Z.-E. Meziani,
TEMPLE UNIVERSITY
J.P. Chen, E. Chudakov, D. Gaskell, J. Gomez, J.-O. Hansen,
D. Higinbotham, C.W. de Jager, J. LeRose,
R. Michaels, S. Nanda, B. Reitz, A. Saha, B. Wojtsekhowski,
THOMAS JEFFERSON NATIONAL ACCELERATOR FACILITY
E.R. Kinney,
UNIVERSITY OF COLORADO
J. Ralston,
UNIVERSITY OF KANSAS
E.J. Beise,
UNIVERSITY OF MARYLAND
J. Calarco,
UNIVERSITY OF NEW HAMPSHIRE
N. Liyanage
UNIVERSITY OF VIRGINIA

The $\gamma n \to \pi^- p$ and $\gamma p \to \pi^+ n$ reactions are essential probes of the transition from meson-nucleon degrees of freedom to quark-gluon degrees of freedom in exclusive processes. The cross sections of these processes are also advantageous, for investigation of the oscillatory behavior around the quark counting prediction, since they decrease relatively slower with energy compared with other photon-induced processes. Moreover, these photoreactions in nuclei can be used to search for the onset of quantum chromodynamics (QCD) phenomena such as color transparency and nuclear filtering effects. We propose to perform singles $\gamma p \to \pi^+ n$ measurement from hydrogen, and coincidence $\gamma n \to \pi^- p$ differential cross section measurements at the quasi-free kinematics from deuterium, ^{4}He and ^{12}C for photon energies between 2.25 GeV to 5.8 GeV at a center-of-mass angle of 90°. Seven different energy settings are needed which can be achieved with 3 different linac energies. The proposed measurement will be carried out in Hall A using a 50 μA electron beam impinging on a 6% copper radiator, a liquid hydrogen and deuterium target, a high pressure helium gas target, a solid ^{12}C target, and the two Hall A HRS spectrometers. Nuclear transparency of the $\gamma n \to \pi^- p$ process from ^{4}He and ^{12}C will be measured, in conjunction with exploring the nuclear dependence of rather mysterious oscillations with energy that the BNL A(p,2p) experiments have indicated.

PACS numbers:

INTRODUCTION

Exclusive processes are essential to studies of transitions from the non-perturbative to perturbative regime of QCD. The differential cross sections for many exclusive reactions [1] at high energy and large momentum transfer appear to obey the quark counting rule [2]. The quark counting rule was originally obtained based on dimensional analysis of typical renormalizable theories. The same rule was later obtained in a short-distance perturbative QCD approach by Brodsky and Lepage[3]. Despite many successes, a model-independent test of the approach, called the hadron helicity conservation rule, tends not to agree with data in the similar energy and momentum region. It has been suggested that contributions from nonzero parton orbital angular momentum could break the hadron helicity conservation rule [4], although these contributions are power suppressed as shown by Lepage and Brodsky [3]. In addition some of the cross-section data can also be explained in terms of non-perturbative calculations [5]. Some recent developments, such as the generalized counting rule proposed by Ji *et al.* [6], the derivation of the quark-counting rule from the anti-de Sitter/Conformal Field Theory (AdS/CFT) correspondence [7], and the machinery to compute the hadronic light front wave functions developed by Brodsky *et al.* [8], have focused interest back on this subject.

In recent years, a renewed trend has been observed in deuteron photo-disintegration experiments at SLAC and JLab [9] - [12]. Onset of the scaling behavior has been observed in deuteron photo-disintegration [11, 12] at a surprisingly low momentum transfer of 1.0 $(\mathrm{GeV/c})^2$ to the nucleon. However, a polarization measurement on deuteron photo-disintegration [13], recently carried out in Hall A at Jefferson Lab (JLab), shows disagreement with hadron helicity conservation in the same kinematic region where the quark counting behavior is apparently observed. These paradoxes make it essential to understand the exact mechanism governing the early onset of scaling behavior.

Towards this goal, it is important to look closely at claims of agreement between the differential cross section data and the quark counting prediction. Historically, the elastic proton-proton (pp) scattering at high energy and large momentum transfer has played a very important role. In fact, the re-scaled 90° center-of-mass pp elastic scattering data, $s^{10}\frac{d\sigma}{dt}$ show substantial oscillations about the power law behavior. Oscillations are not restricted to the pp sector; they are also seen in πp fixed angle scattering [14]; the old [15] as well as the new data [17] (from JLab experiment E94-104) on photo production of charged pions, at $\theta_{cms} = 90°$ also show hints of oscillation about the s^{-7} scaling; see for example Fig. 1. Thus, it is essential to confirm and map out these oscillatory scaling behavior. Using high luminosity experimental facilities such as CEBAF, these oscillatory scaling behavior can be investigated with significantly improved precision. This will also help identify the exact nature and the underlying mechanism responsible for the scaling behavior.

The energy and nuclear dependence of such oscillatory behavior is also crucial in the search for signatures of QCD such as the nuclear filtering effect and CT. By finely mapping out the nuclear transparency over the scaling region it should be possible to test the nuclear filtering effect in a new regime. We also note that the traditionally accepted "Glauber approximation" might be tested in these reactions on nuclei. The recent photo-pion experiment (E94104) also collected data on the $\gamma\ n \rightarrow \pi^-\ p$ process in ^{4}He. This was used to extract the transparency as a function of momentum transfered square $|t|$ by taking the acceptance corrected ratio of pion photoproduction yield from ^{4}He to the yield from ^{2}H and corrected for the transparency of ^{2}H. The transparency results suggest deviations from the traditional nuclear physics picture [18]. The results are consistent with Glauber calculations which include the QCD phenomenon of color transparency (CT). A first indication of CT-like effect in this kind of reaction is interesting and calls for more data with improved statistical precision (specially at the higher momentum transfers), in order to put these results on a firmer basis. The qualitative nature of the CT effect is dramatically different from nuclear filtering. One way or the other, then, the experimental outcome of the scattering on the nuclear targets is expected to be of interest to a wide audience.

In this experiment, we propose to measure the fixed-angle cross-section $\frac{d\sigma}{dt}$ for the $p(\gamma,\pi^+)n$ and $n(\gamma,\pi^-p)$ processes. In particular, we plan to map out the region of $\sqrt{s} = 2.25$ - 3.41 GeV in fine steps. We will also measure the photo-pion transparency with the $n(\gamma,\pi^-p)$ process on a ^{4}He target with improved statistical precision, up to the highest $|t|$ accessible at JLab. In addition we will make the first photo-pion transparency measurement in the scaling region with the $n(\gamma,\pi^-p)$ process on a ^{12}C target. The resolution of this experiment is expected to conclusively test traditional nuclear models, and distinguish between various models based on QCD in the perturbative regime.

The proposal body is organized as following. Section II contains the physics motivations of the proposed measurement, Section III describes the proposed experiment, Section IV contains the beam time request, Section V talks about the collaboration backgrounds and responsibilities and Section VI is the summary.

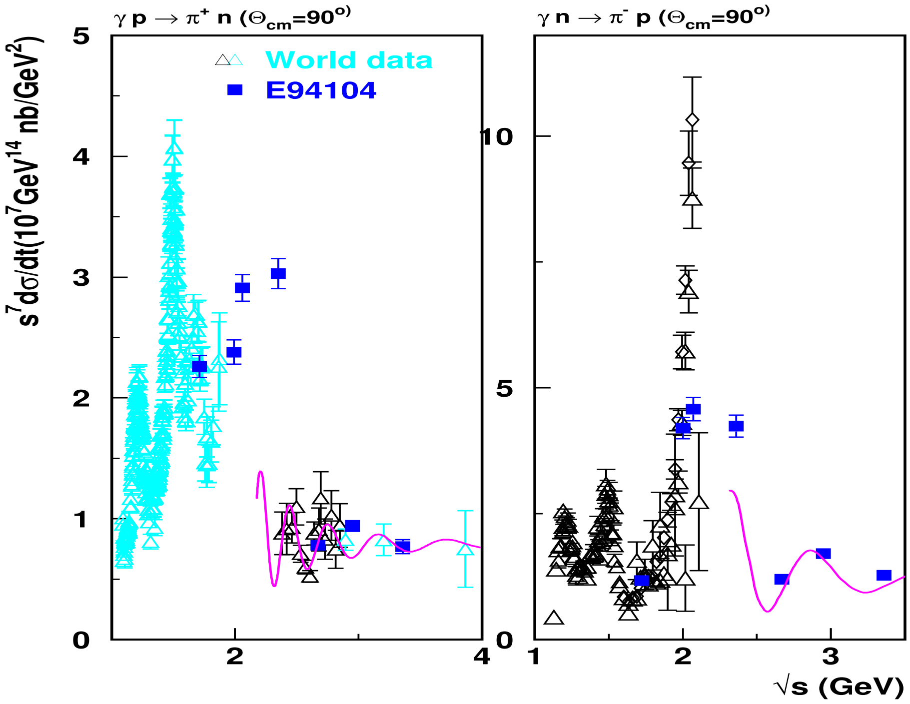

FIG. 1: The scaled differential cross section, $s^7\frac{d\sigma}{dt}$ as a function of $\sqrt{s}$ at a center-of-mass angle of 90°. The left panel is for the $\gamma p \rightarrow \pi^+ n$ channel and the right panel is for the $\gamma n \rightarrow \pi^- p$ channel. The solid curve is a fit based on the two-component model [37]. The open symbols are data from different experiments listed in [16] and the solid symbols are data from E94014 [17].

PHYSICS MOTIVATIONS

Constituent Counting Rule and Oscillations

The constituent counting rule predicts the energy dependence of the differential cross section at fixed center-of-mass angle for an exclusive two-body reaction at high energy and large momentum transfer as follows:

$$d\sigma/dt = h(\theta_{cm})/s^{n-2}, \tag{1}$$

where s and t are the Mandelstam variables, s is the square of the total energy in the center-of-mass frame and t is the momentum transfer squared in the s channel. The quantity n is the total number of elementary fields in the initial and final states, while $h(\theta_{cm})$ depends on details of the dynamics of the process. In the case of pion photoproduction from a nucleon target, the quark counting rule predicts a s^{-7} scaling behavior for $\frac{d\sigma}{dt}$ at a fixed center-of-mass angle. The quark counting rule was originally obtained based on dimensional analysis under the assumptions that the only scales in the system are momenta and that composite hadrons can be replaced by point-like constituents. Implicit in these assumptions is the approximation that the class of diagrams, which represent on-shell independent scattering of pairs of constituent quarks (Landshoff diagrams) [19], can be neglected. Also neglected were contributions from quark orbital angular momentum, which are power suppressed but can give rise to hadron helicity flipping amplitudes. These counting rules were also confirmed within the framework of perturbative QCD analysis up to a logarithmic factor of α_s and are believed to be valid at high energy, in the perturbative QCD region. Such analysis relies on the factorization of the exclusive process into a hard scattering amplitude and a soft quark amplitude inside the hadron. In the last few years an all-orders demonstration of the counting rules for hard exclusive processes has been shown to arise from the correspondence between the anti-de Sitter space and conformal field theory [7] which connects superstring theory to superconformal gauge theory. Although the quark counting rule agrees with data from a variety of exclusive processes, the other natural consequence of pQCD: the helicity conservation selection rule, tends not to agree with data in the experimentally tested region. Hadron helicity conservation arises from quark helicity conservation at high energies and the vector gluon-quark coupling nature of QCD and by neglecting the higher orbital angular momentum states of quarks or gluons in hadrons. The same dimensional analysis which predicts the quark counting rule also predicts hadron helicity conservation for exclusive processes at high energy and large momentum transfers. If hadron helicity conservation holds, the induced polarization of the recoil proton in the unpolarized deuteron photo-disintegration process is expected to be zero. A polarization measurement [13] in deuteron photo-disintegration has been carried out recently by the JLab E89-019 collaboration. While the induced polarization does seem to approach zero around a photon energy of 1.0 GeV at 90° center-of-mass angle, the polarization transfer data are inconsistent with hadron helicity conservation.

The entire subject is very controversial. Isgur and Llewellyn-Smith [5] argue that if the nucleon wave-function has significant strength at low transverse quark momenta ($k_\perp$), then the hard gluon exchange (essential to the perturbative approach) which redistributes the transfered momentum among the quarks, is no longer required. The applicability of perturbative techniques at these low momentum transfers is in serious question. There are no definitive answers to the question- *what is the energy threshold at which pQCD can be applied?* Indeed the exact mechanism governing the observed quark counting rule behavior remains a mystery. Thus, it is crucial to also look for other QCD signatures.

Apart from the early onset of scaling and the disagreement with hadron helicity conservation rule, several other striking phenomena have been observed in pp elastic scattering. One such phenomena is the oscillation of the differential cross-section about the scaling behavior predicted by the quark counting rule (s^{-10} for pp scattering), first pointed out by Hendry [20] in 1973. Secondly, the spin correlation experiment in pp scattering first carried out at Argonne by Crabb *et al.* [21] shows striking behavior: it is ~ 4 times more likely for protons to scatter when their spins are both parallel and normal to the scattering plane than when they are anti-parallel, at the largest momentum transfers (${p_T}^2 = 5.09$ (GeV/c)^2, $\theta_{c.m.} = 90°$). Later spin-correlation experiments [22] confirm the early observation by Crabb *et al.* [21] and showed that the spin correlation A_{NN} (given by $\frac{\sigma(\uparrow,\uparrow)-\sigma(\uparrow,\downarrow)}{\sigma(\uparrow,\uparrow)+\sigma(\uparrow,\downarrow)}$) varies with energy about the pQCD prediction. Theoretical interpretation of this oscillatory behavior of the scaled cross-section ($s^{10}\frac{d\sigma}{dt}$) and the striking spin-correlation in pp scattering was attempted by Brodsky, Carlson, and Lipkin [23] within the framework of quantum chromodynamic quark and gluon interactions, where interference between hard pQCD short-distance and long-distance (Landshoff) amplitudes was discussed for the first time. The Landshoff amplitude arises due to multiple independent scattering between quark pairs in different hadrons. Although each scattering process is itself a short distance process, different independent scatterings can be far apart, limited only by the hadron size. Moreover, gluonic radiative corrections give rise to a phase to this amplitude which is calculable in pQCD [24]. This effect is believed to be analogous to the coulomb-nuclear interference that is observed in low-energy charged-particle scattering. It was also shown that at medium energies this phase (and thus the oscillation) is energy dependent [25], while becoming energy independent at asymptotically high energies [25], [26].

Lastly, Carroll *et al.* [27] reported the anomalous energy dependence of nuclear transparency from the quasi-elastic A(p,2p) process: the nuclear transparency first rises followed by a decrease. This intriguing result was confirmed recently at Brookhaven [28] with improved experimental technique in which the final-state was completely reconstructed. Ralston and Pire [29] explained the free pp oscillatory behavior in the scaled differential cross section and the A(p,2p) nuclear transparency results using the ideas of interference between the short-distance and long-distance amplitudes and the QCD nuclear filtering effect. Carlson, Chachkhunashvili, and Myhrer [30] have also applied such an interference concept to the pp scattering and have explained the pp polarization data. While, Brodsky and de Teramond [40] claimed that the structure seen in $s^{10}\frac{d\sigma}{dt}(pp \to pp)$, the A_{NN} spin correlation at $\sqrt{s} \sim 5$ GeV (around center-of-mass angle of 90°) [21],[22], and the $A(p,2p)$ transparency result can be attributed to $c\bar{c}uuduud$ resonant states. The opening of this channel gives rise to an amplitude with a phase shift similar to that predicted for gluonic radiative corrections.

A number of new developments have generated renewed interest in this topic. Zhao and Close [31] have argued that a breakdown in the locality of quark-hadron duality (dubbed as "restricted locality" of quark-hadron duality) results in oscillations around the scaling curves predicted by the counting rule. They explain that the smooth behavior of the scaling laws arise due destructive interference between various intermediate resonance states in exclusive processes at high energies, however at lower energies this cancellation due to destructive interference breaks down locally and gives rise to oscillations about the smooth behavior. On the other hand, Ji *et al.* [6] have derived a generalized counting rule based on pQCD analysis, by systematically enumerating the Fock components of a hadronic light-cone wave function. Their generalized counting rule for hard exclusive processes include parton orbital angular momentum and hadron helicity flip, thus they provide the scaling behavior of the helicity flipping amplitudes. The interference between the different helicity flip and non-flip amplitudes offers a new mechanism to explain the oscillations in the scaling cross-sections and spin correlations. Brodsky *et al.* [8] have used the anti-de Sitter/Conformal Field Theory correspondence or string/gauge duality [7] to compute the hadronic light front wave functions exactly and it

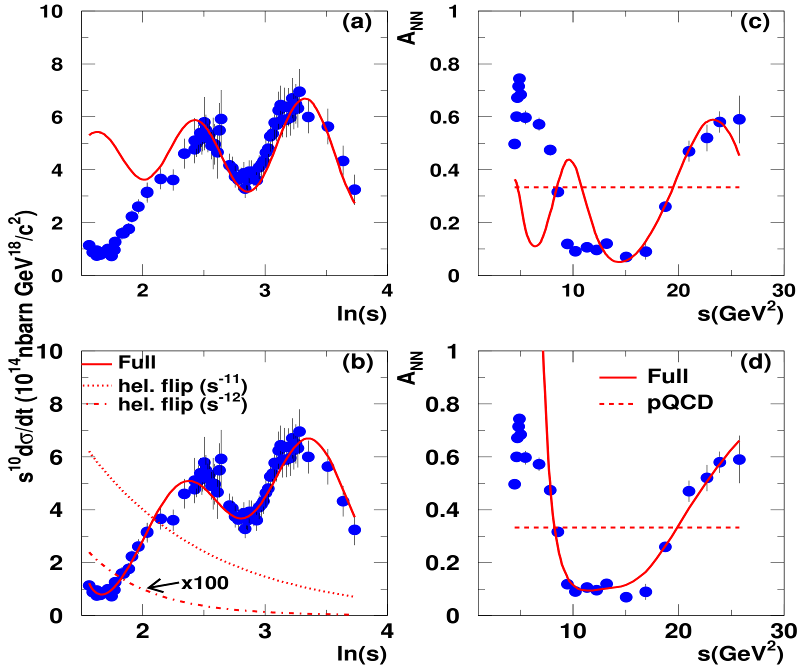

FIG. 2: (a) The fit to pp scattering data at $\theta_{cm} = 90°$ of Ralston and Pire [29]. (b) Fit The same data when the helicity flipping amplitudes are included. The solid line is the fit result, the dotted line is contribution from the helicity flip term $\sim s^{-11}$, the dot-dashed line is contribution from the helicity flip term $\sim s^{-12}$. The $\sim s^{-12}$ contribution has been multiplied by 100 for display purposes. (c) The fit to A_{NN} from polarized pp scattering data at $\theta_{cm} = 90°$ of Carlson *et al.* [30]. (d) Fit to the same data when the helicity flip amplitudes are included. The cross-section data are from Ref. [35] and the A_{NN} data are from Ref. [21, 22].

yields an equivalent generalized counting rule without the use of perturbative theory. In a further test of these new approaches, calculations of the nucleon formfactors including quark orbital angular momentum in pQCD [32] and those computed from light-front hadron dynamics [8] both seem to explain the $\frac{1}{Q^2}$ fall-off of the proton formfactor ratio, $G_E(Q^2)/G_M(Q^2)$, measured recently at JLab in polarization transfer experiments [33].

In addition to these new developments, we have examined [34] the role of the helicity flipping amplitudes in the oscillatory scaling behavior of pp scattering and the oscillations in the spin correlations observed in polarized pp scattering. We noticed that just using the Landshoff amplitude and its interference with the short distance term, fails to describe the data at low energies ($s < 10$ GeV^2). Since the Landshoff amplitude is expected to be significant only at high energies, it is not unreasonable that the above formalism does not describe the data at low energies. We used the generalized counting rule of Ji *et al.* [6] to obtain the scaling behavior of the helicity flipping amplitudes. Our new fit [34] including the helicity flip amplitudes describes the scaled cross-section as well as the spin-correlation data much better specially at the low energies(Fig. 2). The helicity flip amplitudes arising from the parton orbital angular momentum are non-negligible when the parton transverse momentum can not be neglected compared with the typical momentum scale in the exclusive processes. At relatively low energies this is certainly the case, and thus one would expect the helicity flip amplitudes to be a significant contribution to the cross-section at low energies. Moreover, the generalized counting rule of Ji *et al.* predicts a much faster fall-off with energy for the helicity flip amplitudes as expected. An examination of the explicit contribution from the different amplitudes show that the helicity flip amplitudes and their interference are indeed quite significant at low energies and help describe the data at low energies. Results from our fits are shown in Fig. 2. These are very promising results and should be examined for other reactions.

It was previously thought that the oscillatory $s^{10}\frac{d\sigma}{dt}$ feature is unique to pp scattering or to hadron induced exclusive processes. However, it has been suggested that similar oscillations should occur in deuteron photo-disintegration [36], and photo-pion productions at large angles [37]. The QCD re-scattering calculation of the deuteron photo-disintegration process by Frankfurt, Miller, Sargsian and Strikman [36] predicts that the additional energy dependence of the differential cross-section, beyond the $s^{11}\frac{d\sigma}{dt}$ scaling arises primarily from the $n-p$ scattering in the final state. If these predictions are correct, such oscillatory behavior may be a general feature of high energy exclusive photoreactions. Thus it is very important to experimentally search for these oscillations in photoreactions.

Farrar, Sterman and Zhang [38] have shown that the Landshoff contributions are suppressed at leading-order in large-angle photoproduction but they can contribute at subleading order in $\frac{1}{Q}$ as pointed out by the same authors. In principle, the fluctuation of a photon into a $q\bar{q}$ in the initial state can also contribute an independent scattering amplitude at sub-leading order. However, the vector-meson dominance diffractive mechanism is already suppressed in vector meson photoproduction at large values of t [39]. On the other hand such independent scattering amplitude can contribute in the final state if more than one hadron exist in the final state, which is the case for both the deuteron photo-disintegration and nucleon photo-pion production reactions. Thus, an unambiguous observation of such an oscillatory behavior in exclusive photoreactions with hadrons in the final state at large t may provide a signature of QCD final state interaction. The most recent data on $d(\gamma,p)n$ reaction [11, 12] show that the oscillations, if present, are very weak in this process, and the rapid drop of the cross section ($\frac{d\sigma}{dt}\propto\frac{1}{s^{11}}$) makes it impractical to investigate such oscillatory behavior.

Given that the nucleon photo-pion production has a much larger cross-section at high energies ($\frac{d\sigma}{dt}\propto\frac{1}{s^{7}}$), it is very desirable to use these reactions to verify the existence of such oscillations. In fact some precision data on $\gamma p\to\pi^+n$ and $\gamma n\to\pi^-p$ was recently reported by JLab experiment E94-104 [17]. The results indicate the constituent counting rule behavior at center-of-mass angle of 90°, for photon energies above $\sim$ 3 GeV (i.e. above the resonance region). In addition to the s^{-7} scaling behavior, these data also suggest an oscillatory behavior. However, the rather coarse beam energy settings prevent a conclusive statement about the oscillatory behavior. Moreover, the photo-pion production data can also be described similarly by including the helicity flip terms along with the Landshoff terms [34], however because of the coarse energy spacing of the data the results of these new fits are not as illustrative as the pp case. Thus, to verify any structure in the scaled cross-section of photo-pion production processes, it is imperative that we do a fine scan of the scaling region for the $\gamma p\to\pi^+n$ and $\gamma n\to\pi^-p$ processes at a 90° center-of-mass angle.

Nuclear Filtering and Color Transparency

If the oscillations are a persistent feature of hard nucleon scattering, the next natural question that arises is: what is the nuclear dependence of the oscillations? There are established methods for obtaining the expected attenuation in nuclear targets exist. It is argued that large quark separations (long distance amplitudes) tend not to propagate in the strongly interacting nuclear medium, while small quark separations propagate with small attenuation. This leads to suppression of the oscillation phenomena arising from interference of the long distance amplitude with the short distance amplitude. This is dubbed as "nuclear filtering." This nuclear filtering idea is put forward as one of the explainations for the unusual structure in the transparency measured in A(p,2p) experiments carried out at Brookhaven [27]. They observe that the transparency first rises for $Q^2\approx 3$ - 8 (GeV/c)^2, and then decreases at higher momentum transfers, as shown in Fig 3. A more recent experiment [28], completely reconstructing the final-state of the A(p,2p) reaction, confirms the validity of the earlier Brookhaven experiment. If the oscillatory behavior of the cross-section is suppressed in nuclei one would expect to see oscillations in the transparency, which are 180^0 out of phase with the oscillations in the free pp cross-section. This is because the transparency is formed by dividing the A(p,2p) cross-section by the pp cross-section scaled by the proton number Z of the nuclear target. On the other hand as mentioned earlier, Brodsky and de Teramond [40] claim that the structure seen the $A(p,2p)$ transparency result can be attributed to $c\bar{c}uuduud$ resonant states. While interpretations of the elastic $pp\to pp$ cross section, the analyzing power A_{NN} and the transparency data remain controversial, the ideas of nuclear filtering effect and the interference between the hard pQCD short-distance and the long-distance Landshoff amplitudes by Ralston and Pire [29] are able to explain both the $s^{10}\frac{d\sigma}{dt}(pp\to pp)$ oscillatory behavior and the Brookhaven A(p,2p) transparency data. Carlson, Chachkhunashvili, and Myhrer [30] have also applied such an interference concept to explain the pp polarization data.

As mentioned in the introduction, oscillations are suggested by the new cross-section data in photo-pion production reactions. Such oscillatory behavior is predicted from QCD if the independent scattering (Landshoff) regions are important. Nuclear filtering in turn should remove these regions. Thus one can investigate the nuclear filtering effect by measuring transparency in the pion photoproduction reactions on heavy nuclei. Fig. 4 shows the world data (upper panel) and a calculation of the scaled differential cross-section $s^7\frac{d\sigma}{dt}$ for the $\gamma p\to\pi^+n$, as a function of $\sqrt{s}$ at a center-of-mass angle of 90° and the calculated transparency (lower panel) of the $\gamma p\to\pi^+n$ process as a function of $\sqrt{s}$ for heavy targets such as ^{12}C, using a two-component model of Jain, Kundu, and Ralston [37]. There are two different phases in the two-component model: the QCD energy-dependent phase due to the gluon radiation as in the free cross section, and the phase difference between the two amplitudes in the effective nuclear potentials in

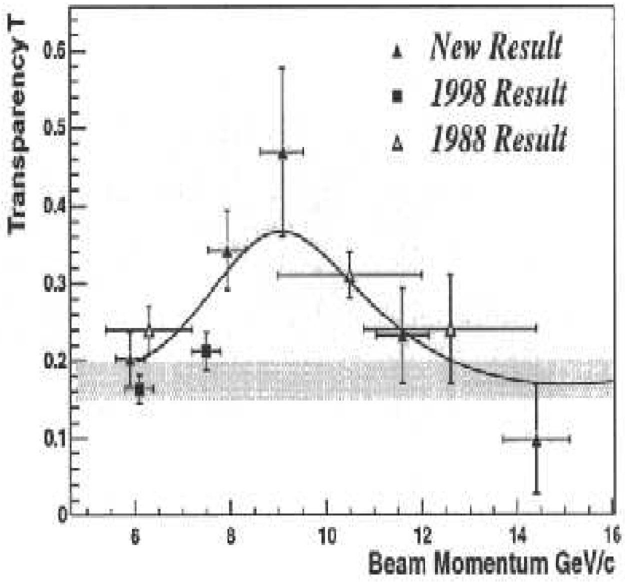

FIG. 3: Nuclear transparency as measured in the A(p,2p) precess on carbon. The shaded band represents the Glauber calculation for carbon and the solid line is the calculation from Ref. [29]

the nuclear medium. While the QCD phase can be determined by fitting the free cross-section, the latter phase is unknown. The results of the two-component model shown are obtained for different values of the second phase. An effective $p-N$ cross section of 30 mb is used in this calculation based on the $A(e,e'p)$ data [45], and the $\pi-N$ cross section is attenuated by $\frac{1}{Q}$ based on the pQCD calculation [41]. Although the calculation was carried out for the $\gamma p \rightarrow \pi^+ n$ channel (where free space cross-section data exists), the following features are expected for the $\gamma n \rightarrow \pi^- p$ channel as well: (i) an overall slow increase in the transparency as $\sqrt{s}$ increases; (ii) an oscillatory behavior with amplitude depending strongly on the relative phase between the effective nuclear potential of the short-distance and the long-distance amplitudes in the nuclear medium. While a relative phase angle of ZERO predicts the smallest amplitude for the oscillation, it is disfavored by the Brookhaven A(p,2p) transparency data [46]. The experimental verification of the nuclear filter effect would be a very interesting confirmation of this QCD based approach in the transition region. For a detailed discussion on the nuclear filtering effect and related subjects, we refer to a review article on the subject [44].

In addition to nuclear filtering the pion-photoproduction process on light nuclei such as ^{4}He can be used to look for the complementary phenomena of Color Transparency. CT, first conjectured by Mueller and Brodsky [42] refers to the suppression of final (and initial) state interactions of hadrons with the nuclear medium in exclusive processes at high momentum transfers, and is a natural consequence of QCD. It is based on the idea that, at sufficiently high momentum transfer, the dominant amplitudes for exclusive reactions involve hadrons of reduced transverse size (dubbed the point like configuration or PLC) which can then pass undisturbed through the nuclear medium. This is a novel QCD phenomenon which, if observed, would be a clear manifestation of hadrons fluctuating to a small size in the nucleus. JLab experiment E94-104, recently reported the first measurement of nuclear transparency of the $\gamma n \rightarrow \pi^- p$ process from ^{4}He [18]. The measured transparency seem to deviate from the traditional nuclear physics predictions at the higher momentum transfers that suggests a CT-like behavior. This is the first indication of CT-like effect in this kind of reaction, however, the statistical precision of the data at the highest energies was poor. A new measurement with better statistical precision in this energy range and extending the measurement to highest energies possible at JLab is crucial for confirming these results.

Recently, a first complete calculation of "color transparency" and 'nuclear filtering' in perturbative QCD has been carried out for electro-production experiments [41]. These calculations show that the nuclear filtering effect is complementary to color transparency (CT) effect. While nuclear filtering uses the nuclear medium actively, in CT large momentum transfers select out the short distance amplitude which are then free to propagate through the passive nuclear medium. In addition, based on the quantum diffusion model by Farrar, Liu, Frankfurt and

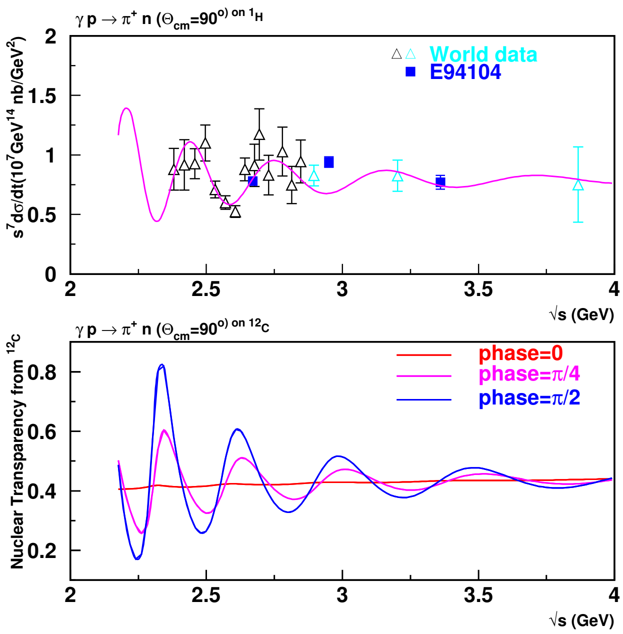

FIG. 4: The upper panel shows world data on the scaled differential cross-section $s^7 \frac{d\sigma}{dt}$ for the $\gamma p \to \pi^+ n$ process, as a function of $\sqrt{s}$ at a center-of-mass angle of 90°. The solid curve is a fit of the data based on the two-component model [37]. The lower panel shows the calculated nuclear transparency of the $\gamma p \to \pi^+ n$ process as a function of cms energy, $\sqrt{s}$ for ^{12}C, in the two-component model [37].

.

Strikman [43], the expansion time of the PLC relative to the time to traverse the nucleus is an essential factor for the observation of the CT effect. Thus, while one expects to observe the onset of CT effect sooner in light nuclei compared to heavier nuclei, the large A limit provides a perturbatively calculable limit for the nuclear filtering effect. This makes ^{4}He and ^{12}C a good choice as the targets for the proposed nuclear transparency measurement. Light nuclei such as ^{4}He are predicted to be better for the search of CT phenomenon because of their relatively small nuclear sizes. The new results from E94-104 [18] also indicate the merits of ^{4}He nuclei in the search for CT. Furthermore, nucleon configurations obtained from the exact nuclear ground state wavefunction are available for ^{4}He [47]. These configurations along with the elementary hadron-nucleon cross-sections can be used to carry out precise calculations of the nuclear transparency [48] in the framework of Glauber theory [49]. Therefore, precise measurement of nuclear transparency from ^{4}He nuclei is a benchmark test of these traditional nuclear calculations and can be used to explore where the calculations start to break down. On the other hand ^{12}C is a good target to look for nuclear filtering as shown by the calculations of Jain *et al.* [37].

The search for CT has been motivated anew by the recent insight that the onset of CT can provide alternative source of information [50] on the generalized parton distributions (GPDs) [51] by mapping out the behavior of the transverse components of the wave-function. The GPDs which were developed in the last few years, provide the relationship between the longitudinal and transverse momentum structure of partons in a fast moving hadron [51]. If the onset of CT and nuclear filtering are experimentally confirmed, because both are sensitive to the transverse size of hadronic configurations, they have the potential to be a powerful means to measure the experimentally elusive GPDs [50, 52]. The impact parameter representation of the GPDs can be used to model the effective size of the knocked out particle in an hard exclusive process [53]. CT can only occur if this effective size is smaller than the mean square radius of the hadron and thus the observation of CT will then constrain the possible analytic behavior of GPDs [52]. Given the tremendous interest generated by this novel formalism of GPDs it is very important to search for CT in reactions, such as photo-pion production on light nuclei, where hints of CT like behavior has been reported [18].

In summary, the preliminary E94-104 results in a rather coarse step of $\sqrt{s}$, seem to suggest oscillatory behavior in the scaled cross-section; $s^7 \frac{d\sigma}{dt}$. Thus, it is essential to confirm such oscillatory behavior by performing a measurement with finer step of $\sqrt{s}$ in the $\gamma p \to \pi^+ n$ and $\gamma n \to \pi^- p$ processes. Furthermore, a nuclear transparency measurement of the $\gamma n \to \pi^- p$ process from a ^{12}C and ^{4}He target will allow the investigation of the nuclear filtering effect and color transparency.

PROPOSED MEASUREMENTS

We propose to carry out a measurement of the photo-pion production cross-section for the fundamental $\gamma n \to \pi^- p$ process from a ^{2}H , ^{4}He and ^{12}C target and for the $\gamma p \to \pi^+ n$ process from a hydrogen target at a center-of-mass angle of 90^o, at $\sqrt{s} \sim 2.25$ GeV to 3.41 GeV in steps of approximately 0.2 GeV. The maximum beam energy requested is 5.8 GeV, in addition six other energies are rquested, however, *all seven energies can be achieved with just 3 different linac energies.* Transparency will be formed by taking the ratio of the production cross-section from ^{4}He and ^{12}C to the production cross-section from ^{2}H. We plan to make individual cross-section measurements with a 2% statistical uncertainty and point-to-point systematic uncertainties of $< 3\%$. This will allow a precision test of the oscillatory behavior in the scaled free cross section. The systematic uncertainties for the transparency measurement will be greatly reduced when we take the ratio of Helium and Carbon to ^{2}H. Thus, for transparency we plan to make measurements with combined statistical and systematic uncertainties of $< 5\%$. For ^{4}He a 2% statistical uncertainty will enable us to confirm the deviations from the Glauber predictions or CT-like behavior seen in the E94-104 data on ^{4}He [18]. Moreover, calculations of Jain *et al.* [37] in this region predict oscillations of the order of 30% for ^{12}C, thus a comined uncertainty of $< 5\%$ should be sufficient to provide evidence for or against the nuclear filtering effect in nuclear photo-pion production processes.

By inter-spacing the proposed data points in between the already reported data from E94-104 [17] to have cut down the request for beam to just 7 different beam energies. We project that this will be sufficient to test the oscillatory behavior and to investigate the nuclear filtering effect. Some of the beam energies can be accommodated by changing the number of passes in the linac, so only three different energy per pass are needed. The beam energy change is the main overhead of this experiment. The frequent beam energy change adds another level of complexity in scheduling the experiment, thus minimizing the number of changes should go a long way towards helping schedule this experiment. Since this experiment is overhead intensive, it is highly desirable to perform it on all targets as one experiment instead of breaking it up into smaller experiments. Moreover, the proposed experiment is a straight-forward measurement, which requires the standard Hall A equipment. Thus, interweaving the running of this experiment with the running of other compatible Hall A experiments can be a practical running scenario for the scheduling of such an experiment.

While the large acceptance detection and a tagged photon capabilities have enormous advantages for many experiments in Hall B, the proposed experiment will only be possible with the unique JLab capability of high luminosity. The proposed momentum range for the coincidence measurement of the $\gamma n \to \pi^- p$ process makes Hall A the only possible place at JLab where such a measurement can be carried out.

THE EXPERIMENT

Overview

The experiment will employ the Hall A cryogenic liquid hydrogen and deuterium targets, the high pressure helium target and the solid target ladder with a carbon foil target along with the Hall A copper radiator. The maximum energy of the bremsstrahlung beam is essentially equal to the electron kinetic energy. The target, located downstream of the radiator, is irradiated by the photons and the primary electron beam. The quasifree kinematics are chosen for the $n(\gamma, \pi^- p)$ and $p(\gamma, \pi^+)n$ processes. The singles measurement will be performed using the left-arm HRS to detect the π^+. The coincidence measurement will be performed using the Hall A right-arm HRS for the π^- detection, and the left-arm HRS for the proton detection. The detector packages for both HRS arms in this experiment will be identical to that used in the recently completed E94-104 experiment. Fig. 5 shows the experimental layout for the proposed experiment.

The $\gamma n \to \pi^- p$ reaction is a two-body process. By either detecting the momentum and the angle of the photo-proton or detecting the momentum and angle of the photo-produced pion, one can determine the incident photon energy. In this experiment, nuclear targets (deuterium ^{4}He and ^{12}C) will be employed instead of a free neutron target which does not exist in nature. Thus, measurement of the momenta and scattering angles of both the proton and the pion are necessary in order to reconstruct the incident photon energy. Other inelastic channel, such as 2π production can be essentially eliminated, since this is a coincidence measurement and only the highest energy protons and pions are detected. This technique has been well established in the recently completed Hall A experiment E94-104. Using the data from E94-104, we have compared the reconstructed photon energy spectrum for a ^{4}He target with Monte

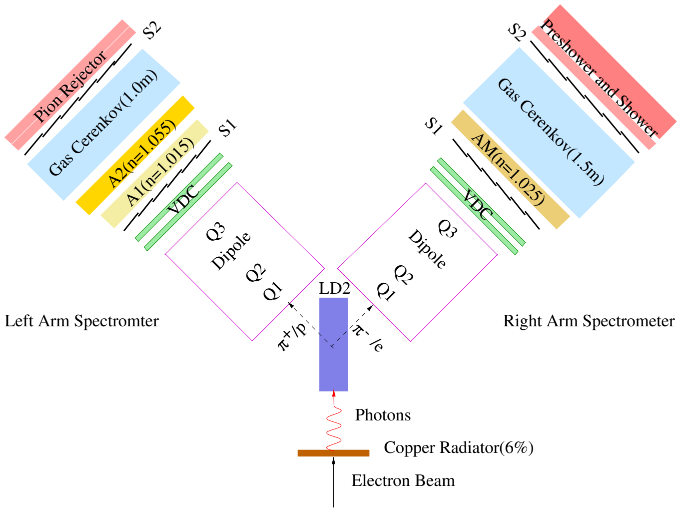

FIG. 5: The proposed experimental layout. The detector packages are identical to what had been used in E94-104.

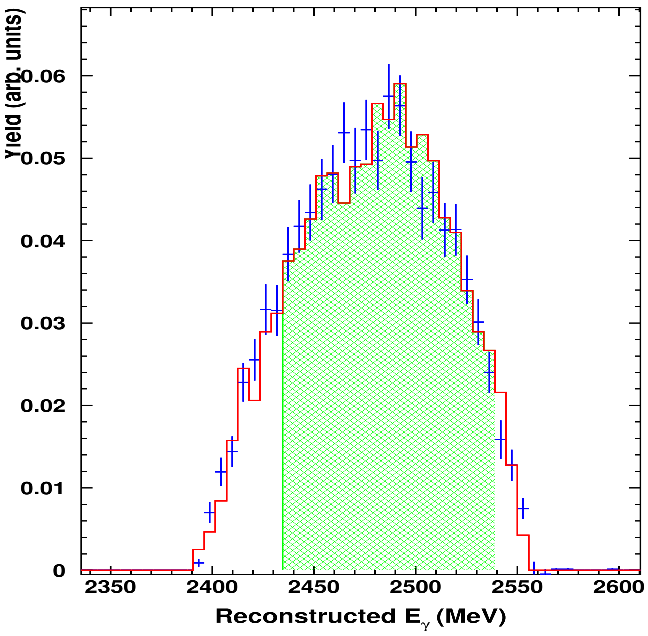

FIG. 6: Reconstructed photon energy spectrum at 2.56 GeV and $\theta_{cm} = 90°$ for a ^{4}He target. The curve is from the Monte Carlo simulation. The shaded area denotes the photon energy region which is used to extract the experimental yield.

Carlo simulation of the same (Fig 6). The excellent agreement between the two gives us added confidence in this technique.

The Electron Beam and the Radiator

An electron beam with a beam current of 50 μA is required for this experiment. The experiment will use a copper radiator of 6% radiation length, which is placed upstream of the target chamber. The copper radiator constructed by the Rutgers University has been used in several completed Hall A photon experiments including the most recent E94-104 experiment.

The proposed running conditions of this experiment are very close to those of E94-104, the background from the

E_{beam}	E_γ	$\sqrt{s}$	θ_{π^+} (lab)	P_{π^+}
GeV	GeV	GeV	deg	GeV/c
2.352	2.277	2.27	44.60	1.3317
2.857	2.782	2.47	41.35	1.5916
3.153	3.078	2.58	39.75	1.7429
3.799	3.724	2.805	36.82	2.0712
4.661	4.586	3.08	33.75	2.5076
5.200	5.125	3.24	32.19	2.7795
5.802	5.727	3.41	30.67	3.0829

TABLE I: Table of kinematics for the $p(\gamma,\pi^+)n$ reaction at pion C.M. angle of 90^o. The photon energy listed is 75 MeV less than the electron beam energy.

copper radiator due to the production of low energy neutrons and high energy pions were demonstrated not to be a problem by E94-104. Another experiment, E00-107 which proposes to use a 50 μA beam has been approved by the PAC.

Target

We plan to use the Hall A liquid deuterium, liquid hydrogen and liquid helium (2% r.l. each) cryotargets and a solid target of carbon (850mg, 2% r.l.). The liquid hydrogen target will be used for the singles $\gamma p \to \pi^+ n$ measurement and for coincidence background studies. The dummy target cell will be used for singles background studies. We propose to run the experiment at a maximum electron beam current of 50 μA, which is significantly below the heat load that the Hall A cryotarget routinely handles. The energy deposited at the highest energy (5.8 GeV) with 50 μA of beam is below the 100 Watts equivalent thick target power limit.

Spectrometer

The two HRS spectrometers will be used to make the coincidence measurement. The right-arm HRS will be used for the π^- detection, and the left-arm HRS for the proton detection. The pion arm momentum setting ranges from 1.32 - 3.08 GeV/c and the angle ranges from 30.7 - 44.8°. The proton arm momentum and angle setting ranges from 1.61 - 3.45 GeV/c and 26.08 - 35.22°. The highest singles rate in the spectrometer is less than 5KHz, which is much lower than the limit for the trigger rate. The left-arm HRS will also be used to detect the π^+ from a hydrogen target.

Background

The dominant background process for this experiment is the quasi-elastic A(e,e'p) reaction. The quasielastically scattered electron has nearly the same momentum and angle as the photo-produced pion in the pion arm, and the scattered proton also has nearly the same momentum and scattering angle as that of the photo-proton in the proton spectrometer. We have estimated the singles ratio of e^-/π^- for the LH2 and LD2 targets, based on the observed ratio in the experiment E94-104. The ratio is < 10 for the LD2 target and < 50 for the LH2 target. The combination of the gas Cherenkov counter, preshower and shower counters can provide an electron rejection factor of 5000, which is sufficient for the proposed experiment. In the proton arm, good particle identification of protons, π^+ particles and positrons is required. The positron background arises from pair production of the bremsstrahlung photons and can be rejected sufficiently using the gas Cherenkov counter because the rate has been estimated to be rather low. Although the π^+ particles from the $\gamma p \to \pi^+ n$ reactions are kinematically eliminated in the proton arm, the π^+ background event can come from multiple processes, which have relatively low rates because of the phase space constraint. The combination of the A1 and A2 aerogel counters will provide more than sufficient π^+ rejection, which has been clearly demonstrated by experiment E94-104. Furthermore, the coincidence requirement effectively suppresses all background channels, except the (e,e'p) channel. Experiment E94-104 demonstrated that the coincidence (e,e'p) background events are sufficiently rejected with the particle identification capabilities provided by the detector packages shown in Fig. 5.

E_{beam}	E_γ	$\sqrt{s}$	θ_{π^-} (lab)	θ_p (lab)	P_{π^-}	P_p
2.352	2.277	2.27	44.60	35.14	1.3317	1.6246
2.857	2.782	2.47	41.35	33.52	1.5916	1.9040
3.153	3.078	2.58	39.75	32.67	1.7429	2.0647
3.799	3.724	2.805	36.82	31.00	2.0712	2.4098
4.661	4.586	3.08	33.75	29.12	2.5076	2.8630
5.200	5.125	3.24	32.19	28.10	2.7795	3.1432
5.802	5.727	3.41	30.67	27.08	3.0829	3.4544

TABLE II: Table of kinematics for the quasifree $n(\gamma, \pi^- p)$ reaction at pion C.M. angle of 90^o. The photon energy listed is 75 MeV less than the electron beam energy.

E_{beam}	$E_\gamma(1)$	$E_\gamma(2)$	$\sqrt{s}(1)$	$\sqrt{s}(2)$
GeV	GeV	GeV	GeV	GeV
2.352	2.302	2.252	2.26	2.28
2.857	2.807	2.757	2.46	2.48
3.153	3.103	3.053	2.57	2.59

TABLE III: Table of central photon energies and $\sqrt{s}$ when the 100 MeV bin between 25 and 125 MeV below the end point energy is divided into 2 bins.This will be done for $\sqrt{s} < 2.8$ GeV.

Kinematics

Tables I and II shows the kinematics for the $p(\gamma, \pi^+)n$ and and the quasifree $n(\gamma, \pi^- p)$ reactions respectively. The photon energy is taken to be 75 MeV below the electron beam energy, since the range of photon energies to be used is a 100 MeV bin from 25 MeV below the end point energy to 125 MeV below the end point energy. However since the rates are relatively high for $\sqrt{s} < 2.8$ GeV, we can divide the 100 MeV bin into two 50 MeV bins for these low $\sqrt{s}$ points. The range in $\sqrt{s} < 2.8$ GeV which is covered by splitting this 100 MeV bin is shown in Table III. The pion center-of-mass angle is 90^o at all settings. The kinematics have been chosen to cover the region between center-of-mass energy $\sqrt{s} = 2.26$ - 3.41 GeV, in steps of approximately 0.2 GeV.

Counting Rates

The counting rate were estimated using the data taken on the ^{2}H and ^{4}He targets during E94104 and a Monte Carlo simulation of the experiment using the Hall A Monte Carlo MCEEP modified for experiment E94-104. The Monte Carlo uses a fit to the existing data on $\gamma n \to \pi^- p$, the measured π^-/π^+ ratio from experiment E94-104 and momentum distributions for ^{2}H, ^{4}He and ^{12}C to simulate the photon energy spectrum for each target (^{1}H, ^{2}H, ^{4}He and ^{12}C respectively). The reconstructed photon energy spectrum for $\gamma n \to \pi^- p$ on a ^{4}He agrees very well with the data, as seen in Fig 6. Similarly we also performed a Monte Carlo simulation for the ^{4}He and ^{12}C targets as shown in Fig 6 and Fig 7. The momentum distribution for ^{12}C was obtained from Hall C experimental data [54]. Using the calculated transparency obtained from Ref [48], we can get an estimate of the relative transparency of ^{12}C with respect to ^{4}He. One can thus obtain the coincidence rates for ^{12}C from this relative transparency using the relation;

$$T_{\text{relative}} = \frac{T_{^{12}C}}{T_{^4He}} = \frac{\text{Data}(^{12}C)/\text{Monte Carlo}(^{12}C)}{\text{Data}(^4He)/\text{Monte Carlo}(^4He)} \tag{2}$$

The relative transparency between ^{12}C and ^{4}He was taken to be 0.8. All rates were estimated for a 50 MeV photon energy window for $\sqrt{s} < 2.8$ GeV and a 100 MeV photon energy window for $\sqrt{s} > 2.8$ GeV, starting 25 MeV below the end point energy. A beam current of 50 μA, a 6% copper radiator and ^{12}C target of thickness 850 mg/cm^2 was used in the estimation. Since the available E94-104 data is more coarsely spaced than this experiment, a linear extrapolation was used to estimate the rates for energies between any two E94-104 data points. The rates for the 15 cm LD2 target were determined from the E94-104 measured rates. The estimated counting rates are shown below in Table IV

The singles $d(\gamma, \pi^-)$ and $d(\gamma, p)$ rates were estimated from the observed singles rates in E94-104. The coincidence timing resolution was taken to be 2 ns in the estimation of the accidental rates. The e$^-/\pi^-$ ratio was estimated from the observed ratio in experiment E94-104. The singles rates, the accidental rates and and the e$^-/\pi^-$ ratio for the

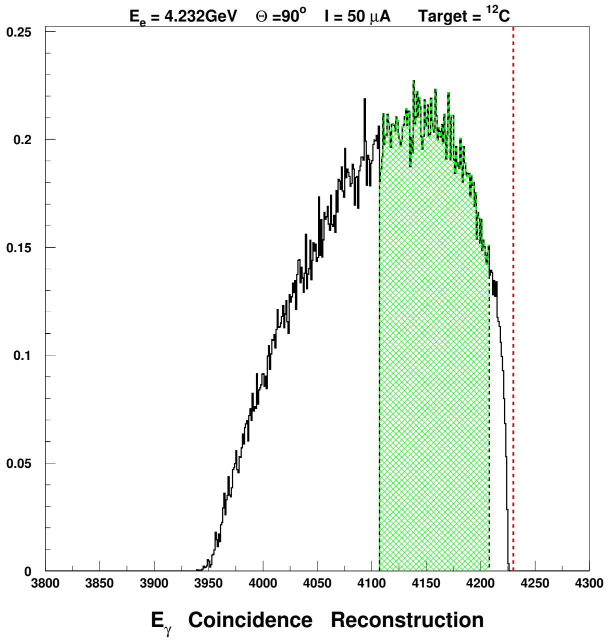

FIG. 7: The Monte Carlo simulation of the reconstructed photon energy spectrum for the ^{12}C target. The shaded region is the 100 MeV window used to determine the rates for $\sqrt{s}$ >2.8 GeV and the red dashed line represents the end point energy.

E_{beam} GeV	$\sqrt{s}$ GeV	LH2 rates Hz	LD2 rates Hz	^{4}He rates Hz	^{12}C rates Hz
2.352	2.27	237.7	30.1	6.62	1.54
2.857	2.47	87.3	12.1	2.42	0.57
3.153	2.58	50.0	6.2	1.44	0.34
3.799	2.81	21.6	2.07	0.54	0.14
4.661	3.08	6.7	1.03	0.21	0.061
5.200	3.24	4.1	0.65	0.11	0.044
5.802	3.41	1.3	0.22	0.062	0.024

TABLE IV: Estimated rates for LH2 (singles), LD2 (coincidence), ^{4}He (coincidence) and ^{12}C (coincidence) in a 50 MeV photon energy window for $\sqrt{s} < 2.8$ GeV and a 100 MeV window for $\sqrt{s} > 2.8$ GeV, starting 25 MeV below the end point energy.

LD2 targets is shown in Tables V. The singles, accidentals and the e^-/π^- ratio are expected to be similar for the solid targets compared to those for the LD2 target.

$\sqrt{s}$ GeV	$d(\gamma,\pi^-)$ rates Hz	$d(\gamma,p)$ rates Hz	accidental Hz	e^-/π^-(LD2)	e^-/π^-(LH2)
2.27	27.5	863.2	8.8E-03	0.45	47.4
2.47	13.0	890.1	4.1E-03	0.51	44.8
2.58	8.3	612.2	2.9E-03	0.60	40.7
2.81	1.6	269.5	0.6E-03	0.75	32.2
3.08	0.77	124.2	0.4E-03	0.81	24.1
3.24	0.4	62.3	1.7E-04	0.95	23.9
3.41	0.2	3.5	1.1E-04	1.01	21.5

TABLE V: Estimated singles rates for LD2 in a 100 MeV photon energy window starting 25 MeV below the end point energy.

$\sqrt{s}$	LH2 beam time	LD2 beam time	^{4}He beam time	^{12}C beam time	Total
GeV	hours	hours	hours	hours	hours
2.27	0.5	0.5	1.0	1.0	3.0
2.47	0.5	0.5	1.0	1.5	3.5
2.58	0.5	0.5	1.0	2.5	4.5
2.81	0.5	0.5	1.5	5.0	7.5
3.08	0.5	1.0	3.5	11.5	16.5
3.24	0.5	1.5	6.5	16.0	24.5
3.41	1.0	3.5	11.5	29.0	45.0
Radiator IN	4.0	8.0	26.0	104.5	142.5
Radiator OUT	2.0	3.0	8.5	35.0	48.5
Bgd Studies	5	10			15
Total					206
Overhead					36+24+10
Grand Total	11.0	21.0	34.5	139.5	276 (11.5 days)

TABLE VI: Estimated beam time requirements for the LH2, LD2, and ^{12}C targets.

Beam Time Estimate

Beam times requirements for data with the radiator were estimated for a goal of 2% statistical uncertainty for the LH2, LD2, ^{4}He and ^{12}C targets. The beam time estimates for the data without the radiator are taken to be a third of the time required with the radiator. The beam time estimates are shown below in table VI. It includes 10 hours of background studies for the coincidence measurement and 5 hours of background studies for the singles measurement. In addition to the 191 hours of beam time listed in the table, we estimate the time for beam energy change [55] for the 7 kinematic points (6 changes) to be an average of 6 hrs each and the overhead for target change from cryo-target to helium target has been estimated to be about 4 hrs each change. Thus the total overhead for beam energy and target change is expected to be around 36+24 hours. All spectrometer setting changes will take place during beam energy changes, thus there are no additional overhead for spectrometer momentum and angle changes. But for the singles measurement, the hadron spectrometer angle and momentum changes and the target and radiator changes will all require an overhead of about 10 hours total for all the 7 kinematic points. Thus, the total overhead is expected to be 70 hours and the total time required for the experiment is 276 hours (11.5 days).

Systematic Uncertainties and Projected Results

The experience gained in E94-104 suggests that the systematic uncertainties of this kind of experiment are well under control. For the cross-section measurements the systematic uncertainties are expected to be $< 5\%$. However, the systematic uncertainty in energy dependence of the cross-section will be $< 3\%$. Since the transparency measurement is a ratio measurement, many of the spectrometer related systematic errors will cancel. We expect the net systematic uncertainty for the transparency measurement to be $< 3\%$. The projected results for LH2, LD2 , ^{4}He and ^{12}C are shown in Fig. 8, Fig. 9, Fig. 10 and Fig. 11. Fig. 11 also shows the calculated transparency [46] for three different phase angles of $0°$, $45°$ and $90°$. It is clear that the projected statistical and systematic uncertainties are more than sufficient to make definitive statements on the predicted oscillations in the scaled cross-section and in the ^{12}C nuclear transparency.

COLLABORATION BACKGROUND AND RESPONSIBILITIES

Many members of the current collaboration have been involved in a number of bremsstrahlung photon beam experiments at SLAC and JLab. Most members of the group are experienced in running the Hall-A radiator, cryotargets and spectrometers. This experiment is a follow-up of experiment E94-104 and most members had participated in that experiment as well as the Hall A photo-proton polarization experiments (E89-019 and E94-012).

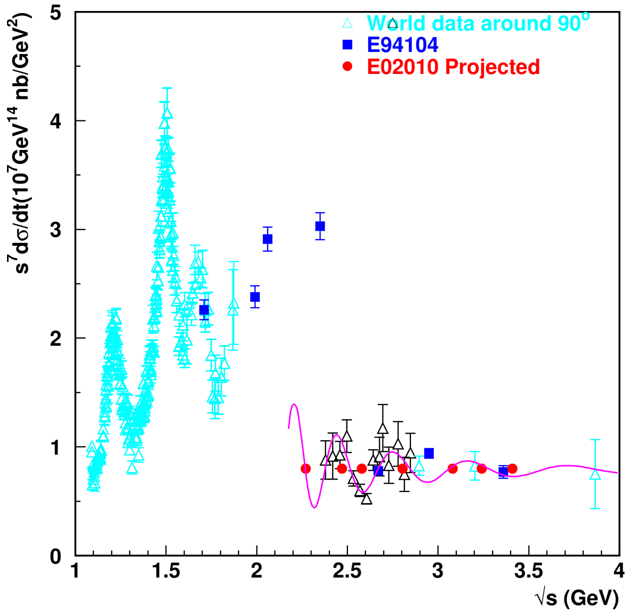

FIG. 8: The scaled differential cross-section $s^7 \frac{d\sigma}{dt}$ for the $p(\gamma, \pi^+)n$ process at C.M. angle of 90°, as a function of cms energy $\sqrt{s}$ in GeV along with the projected measurements for this experiment (red solid points). A 2% statistical uncertainty and a point-to-point 3% systematic uncertainty added in quadrature is shown in the projection.The solid curve is the same as in Fig. 4 (upper panel).

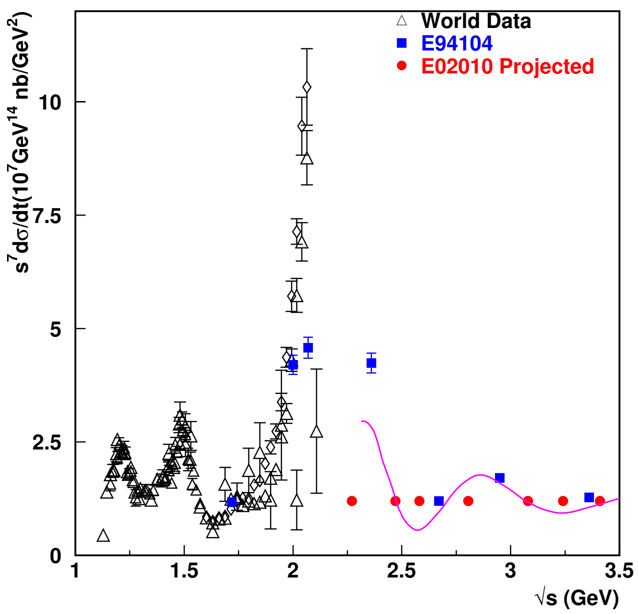

FIG. 9: The projected measurement (red solid points) for the scaled differential cross-section for the process $n(\gamma, \pi^- p)$ as a function of cms energy $\sqrt{s}$ in GeV. A 2% statistical uncertainty and a point-to-point 3% systematic uncertainty added in quadrature is shown in the projection. The solid curve is the same as in Fig. 4 (upper panel).

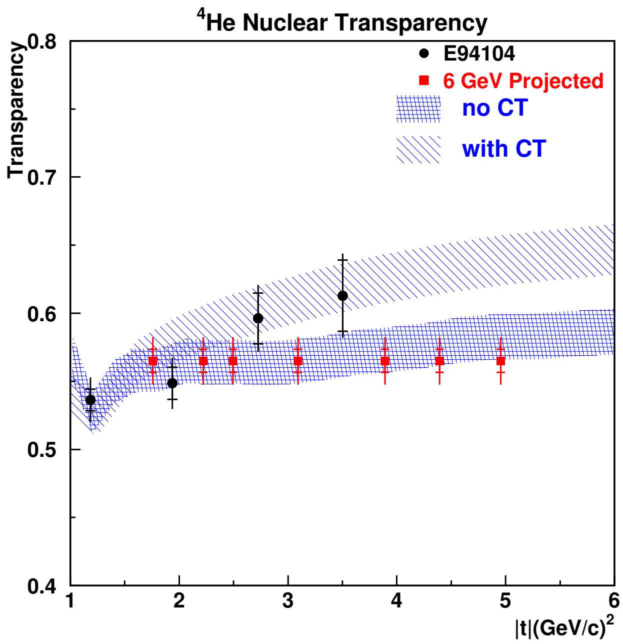

FIG. 10: The predicted nuclear transparency for ^{4}He as a function of momentum transfer squared $|t|$ in (GeV/c)^{2} along with the projected measurements. A 2% statistical uncertainty and a systematic uncertainty of 3% added in quadrature is shown in the projection.

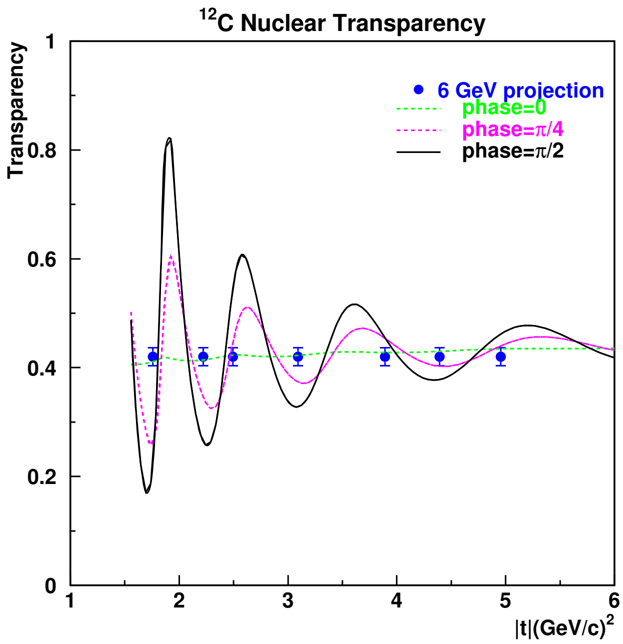

FIG. 11: The predicted nuclear transparency for ^{12}C as a function function of momentum transfer squared $|t|$ in (GeV/c)^{2} along with the projected measurements. A 2% statistical uncertainty and a systematic uncertainty of 3% added in quadrature is shown in the projection. The two-component model prediction by Jain, Kundu and Ralston [37] for phase=0, 45° and 90° are shown as black, green and blue curve, respectively.

SUMMARY

We have proposed a measurement of the $\gamma p \to \pi^+ n$ reaction and $\gamma n \to \pi^- p$ at a center-of-mass angle of 90^o. We plan to map out the region of $\sqrt{s}$ = 2.25 - 3.41 GeV in fine steps of approximately 0.5 GeV. We will also make photo-pion transparency measurement in the scaling region with the $n(\gamma, \pi^- p)$ process at the quasi-free kinematics on a ^{4}He target and the first measurement on a ^{12}C target. These measurements would test the oscillatory behavior of the scaled free space differential cross-sections about the quark counting prediction. And by finely mapping out the nuclear transparency over the scaling region it should be possible to test the ideas of CT and nuclear filtering effect in a new regime. We will use the standard Hall-A equipment along with a 6% copper radiator. The Hall-A cryogenic liquid hydrogen and liquid deuterium and a solid carbon target will be used. A total of 252 hours (10.5 days) of beam time will be required for this experiment.

ACKNOWLEDGEMENTS

We thank G.A. Miller, M. Sargsian and T. W. Donnelly for helpful comments.

[1] C. White *et al.*, Phys. Rev. **D49**, 58 (1994).
[2] S.J. Brodsky and G.R. Farrar, Phys. Rev. Lett.**31**, 1153 (1973); Phys. Rev. D **11**, 1309 (1975); V. Matveev *et al.*, Nuovo Cimento Lett. **7**, 719 (1973);
[3] G.P. Lepage, and S.J. Brodsky, Phys. Rev. D **22**, 2157 (1980).
[4] T. Gousset, B. Pire and J. P. Ralston, Phys. Rev. D **53**, 1202 (1996).
[5] N. Isgur and C. Llewelyn-Smith, Phys. Rev. Lett. **52**, 1080 (1984).
[6] X. Ji, J.-P. Ma and F. Yuan, Phys. Rev. Lett. **90**, 241601 (2003).
[7] J. Polchinski and M.J. Strassler, Phys. Rev. Lett. **88**, 031601 (2002); R.C. Brower and C.I. Tan, Nucl. Phys. B **662**, 393 (2003); O. Andreev, Phys. Rev. D **67**, 046001 (2003).
[8] S. J. Brodsky and G. F. de Teramond, Phys. Lett. **B582**, 211 (2004); S. J. Brodsky *et al.*, Phys. Rev. D **69**, 076001 (2004).
[9] J. Napolitano *et al.*, Phys. Rev. Lett. **61**, 2530 (1988); S.J. Freedman *et al.*, Phys. Rev. C **48**, 1864 (1993); J.E. Belz *et al.*, Phys. Rev. Lett. **74**, 646 (1995).
[10] C. Bochna *et al.*, Phys. Rev. Lett. **81**, 4576 (1998).
[11] E.C. Schulte, *et al.*, Phys. Rev. Lett. **87**, 102302 (2001);
[12] P. Rossi *et al.*, hep-ph/0405207, submitted to Phys. Rev. Letts.; M. Mirazita *et al.*, Phys. Rev. C **70**, 014005 (2004).
[13] K. Wijesooriya, *et al.*, JournalPhys. Rev. Lett.86, 2975 (2001).
[14] D. P. Owen *et al.*, Phys. Rev. **181**, 1794 (1969); K. A. Jenkins *et al.*, Phys. Rev. D **21**, 2445 (1980); C. Haglin *et al.*, Nucl. Phys. B **216**, 1 (1983).
[15] R.L. Anderson *et al.*, Phys. Rev. **D14**, 679 (1976).
[16] "Photoproduction of Elementary Particles", edited by H. Genzel, P. Joos and W. Pfeil pp16-268, (1973).
[17] L. Y. Zhu *et al.*, Phys. Rev. Lett. **91**, 022003 (2003); L. Y. Zhu *et al.*, nucl-exp/0409018.
[18] D. Dutta *et al.*, Phys. Rev. C **68**, 021001 (2003).
[19] P. V. Landshoff, Phys. Rev. D **10**, 1024 (1974).
[20] A.W. Hendry, Phys. Rev. D **10**, 2300 (1974).
[21] D.G. Crabb *et al.*, Phys. Rev. Lett. **41**, 1257 (1978).
[22] G.R. Court *et al.*, Phys. Rev. Lett. **57**, 507 (1986), T.S. Bhatia *et al.*, Phys. Rev. Lett. **49**, 1135 (1982), E.A. Crosbie *et al.*, Phys. Rev. D **23**, 600 (1981).
[23] S.J. Brodsky, C.E. Carlson, and H. Lipkin, Phys. Rev. D **20**, 2278 (1979).
[24] A. Sen, Phys. Rev. D **28**, 860 (1983).
[25] J. Botts and G. Sterman, Nucl. Phys. **B325**, 62 (1989).
[26] A. H. Mueller, Phys. Rep. **73**, 237 (1981).
[27] A.S. Carroll *et al.*, Phys. Rev. Lett. **61**, 1698 (1988).
[28] Y. Mardor *et al.*, Phys. Rev. Lett. **81**, 5085 (1998); A. Leksanov *et al.*, Phys. Rev. Lett. **87**, 212301-1 (2001).
[29] J.P. Ralston and B. Pire, Phys. Rev. Lett. **61**, 1823 (1988), J.P. Ralston and B. Pire, Phys. Rev. Lett. **65**, 2343 (1990).
[30] C.E. Carlson, M. Chachkhunashvili, and F. Myhrer, Phys. Rev. D **46**, 2891 (1992).
[31] Q. Zhao and F. E. Close, Phys. Rev. Lett. **91**, 022004 (2003).
[32] A. V. Belitski, X. Ji and F. Yuan, Phys. Rev. Lett. **91**, 092003 (2003).
[33] M. K. Jones *et al.*, Phys. Rev. Lett. **84**, 1398 (2000); O. Gayou *et al.*, Phys. Rev. Lett. **88**, 092301 (2002).
[34] D. Dutta and H. Gao, hep-ph/0411267
[35] C. W. Akerlof, *et al.*, Phys. Rev. 159, 1138 (1967); R. C. Kammerud, *et al.*, Phys Rev. D **4**, 1309 (1971); K. A. Jenkins, *et al.*, Phys. Rev. Lett, **40**, 425 (1978).

[36] L.L. Frankfurt, G.A. Miller, M.M. Sargsian, and M.I. Strikman, Phys. Rev. Lett. **84**, 3045 (2000), M.M. Sargsian, private communication.
[37] P. Jain, B. Kundu, and J. Ralston, hep-ph/0005126.
[38] G.R. Farrar, G. Sterman, and H. Zhang, Phys. Rev. Lett. **62**, 2229 (1989).
[39] E. Anciant *et al.*, Phys. Rev. Lett. **85**, 4682 (2000).
[40] S. J. Brodsky, and G. F. de Teramond, Phys. Rev. Lett. **60**, 1924 (1988).
[41] B. Kundu, J. Samuelsson, P. Jain and J.P. Ralston, Phys. Rev. D **62**, 113009 (2000).
[42] S.J. Brodsky and A.H. Mueller, Phys. Lett. **B 206**, 685 (1988).
[43] G.R. Farrar, H. Liu, L.L. Frankfurt, and M.I. Strikman, Phys. Rev. Lett. **61**, 686 (1988).
[44] P. Jain, B. Pire, and J.P. Ralston, Phys. Rep. **271**, 67 (1996).
[45] N.C.R. Makins *et al.*, Phys. Rev. Lett. **72**, 1986 (1994); T.G. O'Neill *et al.*, Phys. Lett. **351**, 87 (1995); D. Abbott, *et al.*, Phys. Rev. Lett. **80**, 5072 (1998); K. Garrow, *et al.*, Submitted to Phys. Rev. C.
[46] P. Jain, private communication.
[47] A. Arriaga, V. R. Pandharipande and R. B. Wiringa, Phys. Rev. C **52**,2362 (1995).
[48] H. Gao, R. J. Holt and V. R. Pandharipande, Phys. Rev. C **54**, 2779 (1996).
[49] R. J. Glauber, in *Lectures in Theoretical Physics*,edited by W. E. Brittin *et al.*, (Interscience, New York, 1959).
[50] S. Liuti and S. K. Taneja, hep-ph/0405014.
[51] X. Ji, Phys. Rev. Lett. **78**, 610 (1997); Phys. Rev. D **55**, 7114 (1997); A.V. Radyushkin, Phys. Lett, **B380**, 417 (1996); Phys. Rev. D **56**, 5524 (1997).
[52] M. Burkardt and G. A. Miller, hep-ph/0312190.
[53] M. Burkardt, Int J.. Mod. Phys. A **18**, 173 (2003).
[54] D. Dutta, Ph.D. Thesis, Northwestern University, Unpublished, (1999).
[55] H. Areti, private communication.
[56] M. A. Shupe *et al.*, Phys. Rev. D. **19**, 1921 (1979).